AUTOMATED ESTIMATION OF THE BIOPHYSICAL TARGET FOR RADIOTHERAPY TREATMENT PLANNING USING MULTIMODALITY IMAGE ANALYSIS

Issam El Naqa, Deshan Yang, and Joseph O Deasy

Department of Radiation Oncology, Washington University, School of Medicine, St. Louis, MO 63110

ABSTRACT

In radiotherapy treatment planning of cancer patients, the collection of multiple images of different and yet complementary information is rapidly becoming the norm. Beside CT data sets, PET and/or MRI or MRS images are also being used to aid in the definition of the target volume for treatment optimization. We are investigating methods to integrate available information for joint target registration and segmentation of multi-modality images as perceived by the human observer. Towards this goal, we are exploring multi-valued level set deformable models in conjunction with human perception models for simultaneous delineation of multi-modality images consisting of combinations of PET, CT, or MR datasets. Information from multimodality image sets is integrated based on a logical model to define the final target volume. The methods were demonstrated qualitatively on patient cases of lung cancer with PET/CT and a prostate patient case with CT and MR. We used a series of phantom data of CT, PET, and MR for quantification analysis. Phantom studies suggest 90% segmentation accuracy and less than 2% volume error when integrating all of the three modalities. This is compared with 74% accuracy and 4.4% volume error when using CT-based systems. These results indicate that this semi-automated multimodality-based definition of the biophysical target would provide a feasible and accurate framework for integrating complementary imaging information from different modalities and potentially a useful tool for optimizing of cancer patients radiotherapy plans.

Keywords: Multimodality imaging, segmentation, active contours, human-machine interaction, treatment planning

1. INTRODUCTION

Recently, there has been a burgeoning interest in using different imaging modalities to delineate target volumes and organs at risk in radiotherapy treatment planning [1, 2]. Typically, a trained physician would perform the cumbersome structures delineation by hand because of lack of reliable (semi-) automated image segmentation techniques [3]. We have devised methods based on active contours to improve CT or PET imaging analysis [4, 5], however, single images either CT or PET tend not to carry the whole story, especially in the case of a complex disease like cancer. The Tumors boundaries are not always distinguishable by their Hounsfield numbers on CT nor only by their metabolic activity on PET. Moreover, tumors tend to have heterogeneous textures. Therefore, we define here the so called 'biophysical target', which could be thought of as a mapping from the imaging space to the radiologists/oncologists 'perception' space of the target boundary:

$$\text{Biophysical target} = f(CT, PET, MRI, ...; \lambda), \qquad (1)$$

where $f(\cdot)$ is the mapping function from the different imaging modalities to the target space parameterized by λ, which represents user's defined set of parameters representing his/her prior knowledge. Characterization of the mapping in (1) constitutes a challenging task because it relies on human higher-level expertise that needs to be translated into primitives that a computer algorithm can understand.

In this work, we propose to use a generalization of the geometric deformable model known as the multi-valued level set (MVLS) method as our computational vehicle [6, 7]. We combine the MVLS with a logical model based on user's expertise to approximate the functional in Eq. (1). This process is currently conducted manually by contouring the different modalities separately and attempting to guess the 'true' combined target. The variational nature of the approach would further allow for incorporating smoothness constraint and other prior information, which would make them more robust to image noise and boundary gaps. Moreover, the multimodality structure allows the algorithm to work well in the presence of non-uniform uptakes, partial volume effects, and small mis-registration errors. Besides enjoying the typical characteristics of the level set method such as topological adaptation and inherited subpixel accuracy due to their continuum spatial nature. The method is demonstrated qualitatively and quantitively using clinical and phantom data as discussed in the following sections.

2. METHODS AND MATERIALS

2.1. Data sets

The proposed method was evaluated using 2 sets of clinical data from different cancer sites and a physical phantom data.

2.1.1. Clinical data

The method is demonstrated qualitatively using patient cases of non-small cell lung caner with FDG-PET/CT data, and prostate patient with CT/MR. Only qualitative evaluation was conducted here to avoid statistical bias due to inter- and intra-observer variability in contouring tumors. In the lung case, the data was acquired using an integrated PET/CT machine, where the PET had 5.2x5.2x3.4mm spatial resolution and the CT had 0.98x0.98x5 mm. In the case, of the prostate cancer, the CT had a spatial resolution of 0.71x0.71x3 mm, while the MR had a spatial resolution of 0.78x0.78x10 mm. The MR image we used was T1-weighted. The quality of the delineation was judged visually by experienced oncologists. Quantitative analysis is described next.

2.1.2. Physical phantom data

The commercial phantom is a plastic anthropomorphic head of average human size. Targets consisting of plastic spheres and rods were placed throughout the cranium section of the phantom. Tap water was used for CT imaging. However, for MRI and PET imaging, the water inside the phantom was doped with $CuNO_3$ and ^{18}F-FDG, respectively. The cold spots spheres were considered as the segmentation targets (four spheres each is 25.4 mm in diameter (8.58 mL)). The rods were used as landmarks to assist in alignment. The CT data was digitized at 0.94x0.94x3 mm, PET data at 2.57x2.57x2.57 mm, and MR at 0.98x0.98x2 mm.

2.2. Proposed method for estimation of the biophysical target by concurrent multimodality segmentation algorithm

The algorithm consists of four basic steps: (1) pre-processing image enhancement, (2) co-registration of multimodality images, (3) definition of the logical model parameters, and (4) application of the MVLS algorithm for concurrent segmentation of the used multimodality images.

2.2.1. Co-registration

We used a rigid body co-registration scheme based on normalized mutual information prior to segmentation to refine patient setups misalignment in PET/CT and the rescaling in MR/CT [8]:

$$NMI = \frac{H(A) + H(B)}{H(A,B)}, \tag{2}$$

where $H(\cdot)$ is Shannon entropy.

2.2.2. Multimodality image segmentation by the level set method

The problem of spatial neighborhood definition encountered in clustering methods typically used in such multi-spectral analysis is inherently ameliorated in active contour methods. However, the generalization to multi-imaging modality is based on redefining the concept of boundary as a logical combination of multiple images that mimics human perception. For this seek we used the approach of vectorized or multi-valued level set (MVLS) approach [6, 7]. The solution to the level set problem is found by iteratively by solving the following partial differential equation (PDE):

$$\frac{\partial \phi}{\partial t} = V(\kappa)|\nabla \phi| + F(\Theta), \tag{3}$$

where ϕ is an implicit function (e.g., a signed distance) that represents the evolving level set, (at the boundary contour $\phi(C) = 0$. V is a velocity function proportional to the curvature and inversely proportional to the image gradient. $F(\Theta)$ is a constraint that is typically used to further refine the performance of the algorithm and could be modified to include shape priors and spring forces. Following [6], we used an approach based on the Mumford-Shah model. In this case, the level set method for multi-modality segmentation of *N* images could be formulated as:

$$\inf_C J(C, c^+, c^-) \propto \frac{1}{N}\sum_i \frac{\lambda_i^+ \int_\Omega |I_i - c_i^+|^2 H(\phi) d\mathbf{x} + }{\lambda_i^- \int_\Omega |I_i - c_i^-|^2 (1 - H(\phi)) d\mathbf{x}}, \tag{4}$$

where H is the Heaviside function, $c_i^+ (c_i^-)$ corresponds to the means inside (outside) the contour, and $(\lambda_i^+, \lambda_i^-)$ are user-defined parameter pairs providing 'importance weights' for each of the imaging modalities in comparison with the other modalities. There are various logical combinations of images to capture the underlying biophysical target. In our case, we have chosen to apply, what we denote as a *soft*-AND model. Thus, in this *soft*-AND model, the logical combination of the images is determined by assigning the weights $\lambda_i^\pm$ by experienced in Eq. (3). Currently this is done interactively; however, we are investigating regression methods for automated prediction of these weights depending on the features of the cancer site. The *soft*-AND model could be regarded as a compromise between using a restricted AND model that would only emphasize similar features between the images and an OR model, which tends to be too flexible allowing probably irrelevant features to be included.

After the logical model parameters were assigned, the MVLS algorithm starts by some initial contour in the multi-image domain, then the curve evolves under the influence of the internal (contour curvature and string force) and external forces until equilibrium is reached.

3. EXPERIMENTAL RESULTS

3.1. Application to clinical multimodality data

The biophysical target was identified as the pathological tumor in the PET/CT lung case, and the prostate organ in the MRI/CT case.

In the case of the lung PET/CT shown in Fig 1, the data were collected off an integrated PET/CT machine; moreover, we applied a rigid body mutual information algorithm to correct for small patient misalignments, where NMI improved slightly from 1.21 to 1.22. The PET image was corrected for motion artifacts using a deconvolution method. We selected the larger tumor (right one) for multi-modality analysis. In Figure 1b, we initialize the MVLS algorithm with a generic circle (in black) of 15.4 mm diameter. In Fig. 1c, we show the curve evolution in steps of 10 iterations and the final estimated contour (in thick red). The MVLS algorithm converged in 120 iterations in few seconds.

The analysis of prostate MRI/CT is more challenging because of lack hardware registration and small contrast difference between the prostate and surrounding normal tissues. In Figure 2a we show checkerboard of the co-registration process T1-MRI/CT using rigid body mutual information (MI) algorithm. NMI improved significantly in this case from 1.07 to 1.11. The results of this example seems to be more dependent on initial shape, therefore, the initial contour was emphasized in the algorithm as a prior knowledge. In Fig. 2b, we show the curve evolution in steps of 10 iterations and the final estimated contour (in thick red). The algorithm converged after 50 iterations. In both of the lung and the prostate cases, the delineated biophysical target appeared to agree well with human perception of the 'truth'.

3.2. Quantitative validation using physical phantom data

The phantom data was first co-registered using the CT data as reference. CT is typically used for clinical treatment planning of patients and hence it was selected as a benchmark. The NMI between CT and MR was 1.22 and between CT and PET was 1.28 (see Figure 3a). For validation of segmentation quality, we adopted a spatial overlap index known as the Dice similarity coefficient (DSC) to evaluate the algorithm performance with respect to the known phantom dimensions. We prefer this metric to reporting volumes only, as commonly practiced, because it takes into account the spatial dependency. The segmentation results in terms of DSC (Figure 3b) and volume estimation error (Figure 3c) of the four balls.

The average DSC for PET/CT/MR was estimated to be 90% suggesting excellent segmentation performance (22% improvement over using CT alone) and the error in estimated volume is 1.3% (74% error reduction compared with CT).

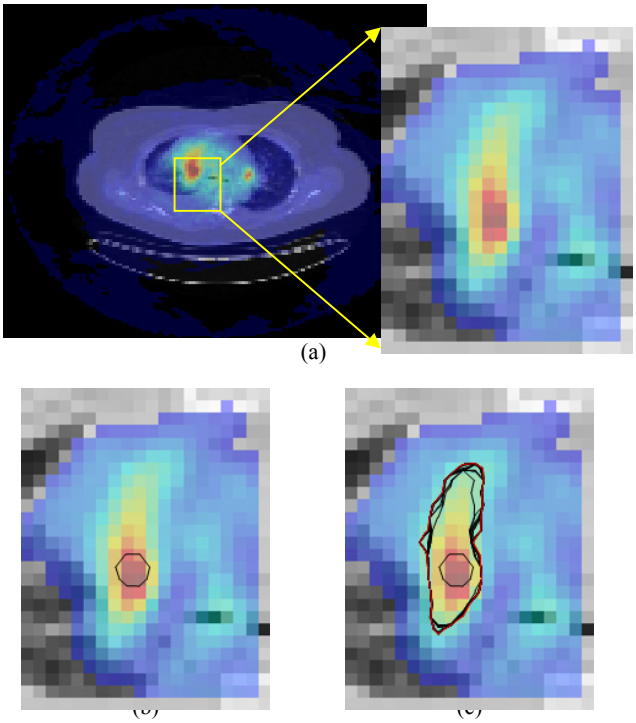

Figure 1. Analysis of lung PET/CT. (a) Co-registered PET/CT, (b) The MVLS algorithm is initialized with a circle (in black) of 15.4 mm diameter, (c) Curve evolution in steps of 10 iterations and the final estimated contour (in thick red).

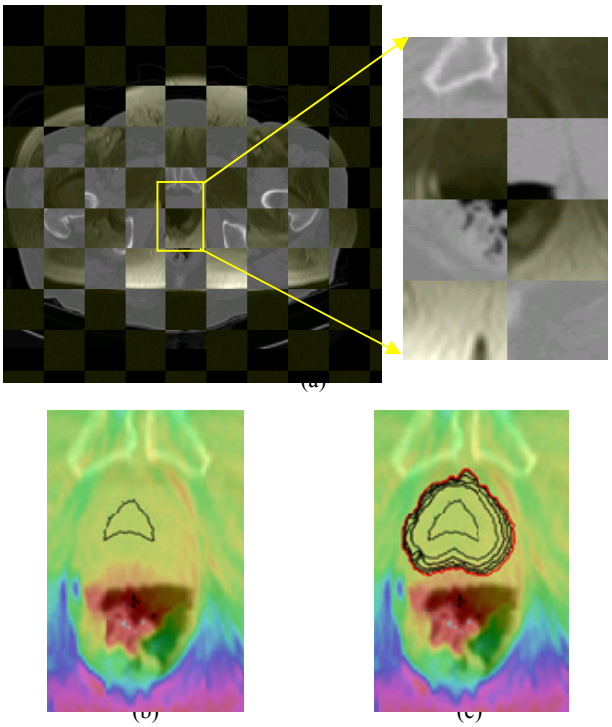

Figure 2. Analysis of prostate MRI/CT. (a) Co-registered MRI/CT and selected ROI, (b) The MVLS algorithm is initialized with a shape prior that roughly resembles prostate (in black), (c) Curve evolution in steps of 10 iterations and the final estimated contour (in thick red).

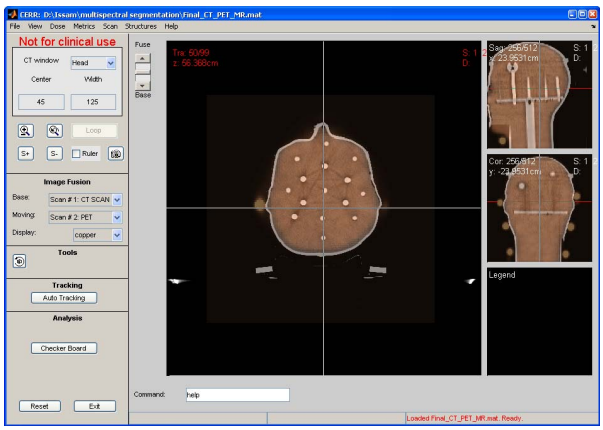

(a)

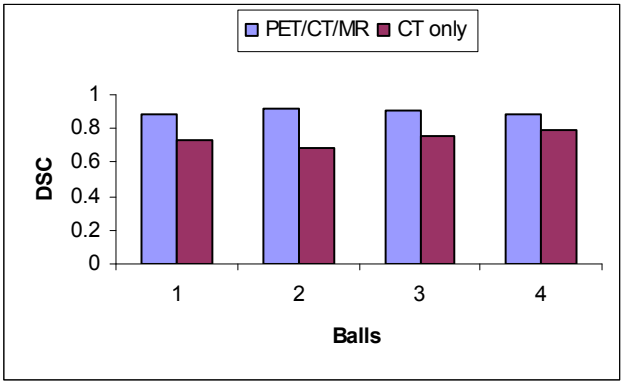

(b)

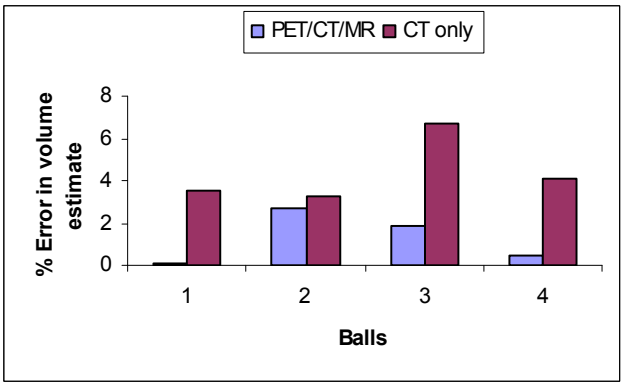

(c)

Figure 3. Physical phantom validation. (a) Registration of the multimodality phantom in CERR (rods were used to evaluate alignment and the balls to evaluate the quality of segmenting the combined PET/CT/MRI data). Estimated segmentation accuracy in terms of (b) DSC and (c) percentage error in estimated volume.

4. CONCLUSIONS

In this work, we have demonstrated a new approach to semi-automatically estimate the biophysical target in radiotherapy treatment planning by integrating information from different multimodality images. The method relies on combining multi-valued level set active contours model with a logical human perception model. The current logical model could be tuned by changing the weights of the different images regionally in accordance with the user's experience. Increasing the number of images would improve the capturing of the contour boundary of the biophysical target. Our simulations on patients' data and physical phantoms indicate that the algorithm results are promising and could provide radiologists/oncologists with reliable and efficient tools to analyze simultaneously different modality data in different cancer sites. However, further intra- and inter-observer variability analyses are required for validation. We hope this data will be ready by the time of the meeting.

5. ACKNOWLEDGEMENTS

This research was partially supported by a grant from the American Cancer Society IRG-58-010-50.

6. REFERENCES

[1] J. D. Bradley, C. A. Perez, F. Dehdashti, and B. A. Siegel, "Implementing biologic target volumes in radiation treatment planning for non-small cell lung cancer," *J Nucl Med*, vol. 45, pp. 96S-101S, 2004.

[2] S. Milker-Zabel, A. Zabel-du Bois, M. Henze, P. Huber, D. Schulz-Ertner, A. Hoess, U. Haberkorn, and J. Debus, "Improved target volume definition for fractionated stereotactic radiotherapy in patients with intracranial meningiomas by correlation of CT, MRI, and [68Ga]-DOTATOC-PET," *IJROB*, 2006.

[3] K. J. Biehl, F. Kong, F. Dehdashti, J. Y. Jin, S. Mutic, I. El Naqa, B. Siegel, and J. Bradley, "18F-FDG PET Definition of Gross Tumor Volume for Radiotherapy of Non-Small Cell Lung Cancer: Is a Single Standardized Uptake Value Threshold Approach Appropriate?," *J Nucl Med*, vol. 47, pp. 1808-1812, 2006.

[4] I. El Naqa, J. Bradley, J. Deasy, K. Biehl, R. Laforest, and D. Low, "Improved Analysis of PET Images for Radiation Therapy," 14th ICCR , Seoul, Korea, 2004.

[5] I. El Naqa, D. A. Low, S. Wahab, P. Parikh, M. Nystrom, J. Hubenschmidt, J. O. Deasy, i. A. Amin, G. Christensen, and J. Bradley, "Automated 4-D Lung Computed Tomography Reconstruction During Free Breathing for Conformal Radiation Therapy," SPIE proceedings, 2004.

[6] T. F. Chan, B. Y. Sandberg, and L. A. Vese, "Active Contours without Edges for Vector-Valued Images," *Journal of Visual Communication and Image Representation*, vol. 11, pp. 130-141, 2000.

[7] J. Shah, "Curve evolution and segmentation functionals: application to color images," 1996.

[8] P. Viola, "Alignment by Maximization of Mutual Information," in *Electrical Engineering and Computer Science*, vol. Ph.D. Cambridge: Massachusetts Institute of Technology, 1995.